Mid- and Near-IR Electronic Absorption Spectrum of CoO Isolated in Solid Neon. Vibronic Data for Low-Lying Electronic States

Delphine Danset and Laurent Manceron*

LADIR/Spectrochimie Moléculaire CNRS UMR 7075, Université Pierre et Marie Curie, case 49, 4 place Jussieu 75252 Paris, France

Received: June 21, 2003; In Final Form: October 1, 2003

The optical absorption spectrum of cobalt monoxide generated by reaction of cobalt atoms and oxygen molecules in solid neon at 4 K has been reinvestigated. New data relative to four low-lying electronic states at 0.42, 0.73, 0.87, and 1.26 eV have been obtained in the mid- to near-IR region, each displaying vibronic structure. If assignment of the second low-lying electronic state to $A^4\Pi_{7/2}$ can be made clearly following previous gas-phase results, assignments of the first, third, and fourth electronic states to $B^4\Sigma$, $a^6\Delta$ and $b^2\Delta$ are tentative and suggested in comparison with existing quantum chemical calculations. For all states vibrational frequencies have been measured and an empirical correlation between CoO bond force constant and internuclear distance, using Herschbach and Laurie's relationship, is proposed.

Introduction

In the last two decades, the CoO molecule has been the object of many spectroscopic studies. Green et al.[1] were among the first to present spectroscopic data on this molecule using isolation in solid argon ($\nu_e = 846.4$ cm^{-1}). Earlier, Weltner et al.[2] had suggested a $^4\Delta$ ground state, based on the absence of ESR activity for matrix-isolated CoO. Proof of a $^4\Delta$ ground state was later given by Adams et al.[3] through a fluorescence study of the red system of gaseous CoO, also deriving a ground-state bond length (1.631 Å) and vibrational frequency ($\nu_0 = 851.7$ cm^{-1}). A detailed examination of the hyperfine and spin−orbit structure of the ground state was done by Clouthier et al.,[4] who obtained hyperfine parameters, established a $(4s\sigma^2)(3d\delta^3)(3d\pi^2)$ electronic configuration and presented an accurate value of 304.3 cm^{-1} for the $^4\Delta_{(5/2-7/2)}$ ground-state separation. These conclusions and spectroscopic constants were further refined in the recent work of Namiki and Saito.[5] Ram et al.[6] were the first to report on the $^4\Pi$ excited state of CoO through a FTIR emission spectroscopy study in the gas phase. A rotational analysis provided $T_0 = 5513.95$ cm^{-1} and $B_0 = 0.4875$ cm^{-1}. From the observation of a large Ω-doubling on some spin−orbit components, it was also suggested in that paper that a $^4\Sigma$ state should lie not too far beneath. Barnes et al.,[7] using Doppler-limited intracavity spectroscopy and jet-cooling methods, reinvestigated the spectrum of CoO in the visible region. Five new allowed electronic transitions ranging from 430 to 720 nm were analyzed and vibrational, rotational, and spin−orbit structures resolved for most states. The existence of other new, low-lying electronic states in the near- and mid-IR was also suggested.

Quantum chemical calculations have been performed for CoO and have met an array of difficulties arising from the near degeneracy of metal 3d or 4s and oxygen 2p atomic orbitals, as well as the importance of electron correlation treatment. Contradicting Krauss and Stevens,[8] Dolg et al.[9] calculated a $^4\Delta$ ground state arising from the $\sigma^2\delta^3\pi^2$ configuration and a $^4\Sigma^-$ state, with a $\sigma\delta^4\pi^2$ configuration, lying about 0.5 eV above. Later, Bauschlicher and Maitre[10] confirmed a $^4\Delta$ ground state at the CCSD(T) level. More recently, several groups applied DFT methods. Bridgeman and Rothery's[11] results were unable to reproduce the correct ground state, unlike Gutsev et al.,[12] who found a $^4\Delta$ ground state and a $^4\Sigma^-$ state lying 0.11 eV above. Uzunova et al.,[13] using the B1LYP exchange-correlation functional calculated several CoO excited states, lying within 1 eV of the ground state. Though the first calculated excited state is the $^4\Sigma^-$, in good agreement with the experimental suggestions, two intriguing points arise from their results. The first is that the calculated bond length for the $^4\Sigma^-$ state is shorter than that of the $^4\Delta$ ground state, and the second is that the $^4\Pi$ state does not appear in this energy range. The latest work is that of Dai et al.[14] using DFT and TDDFT methods, they calculated energies and electronic configurations for the ground and excited states of all first-row transition-metal monoxides. The lack of prediction of bond lengths or frequencies impairs a further check of their predictions for excited states, and the calculated bond length for the ground state is in poor agreement with experimental results.[4,5]

In this paper we present new experimental evidence for four vibronic systems of CoO, isolated in solid neon at 4 K, using FT absorption spectroscopy. Though matrix isolation quenches effects due to rotation, it simplifies greatly the spectral analysis and can also provide an overview of relative intensities for electronic and vibrational transitions spanning a broad spectral range; in the present case, our investigations cover from 80 to 30 000 cm^{-1}.

Experimental Section

The CoO molecules were prepared by cocondensing Co vapor and dilute O_2−Ne mixtures (200−2000 ppm O_2 in Ne), onto one of six flat, Rh-plated copper mirrors maintained at less than 3.5 K using a pulse tube closed-cycle cryogenerator (Cryomech PT405). A 50 K brass radiation shield was fitted to the first stage of the cryogenerator. A second, concentric copper shield, fitted to a liquid nitrogen trap, limited the thermal load to about 150 mW from three 12 mm-diameter holes placed to allow deposition, irradiation, and optical analysis. The setup was

* To whom correspondence should be addressed. E-mail: lm@ccr.jussieu.fr.

10.1021/jp0357626 CCC: $25.00
Published on Web 11/25/2003

evacuated at about 7×10^{-8} mbar before refrigeration of the sample holder. The gas inlet line was driven through the liquid nitrogen trap within the vacuum system, thereby condensing all undesired impurities in the mixture and precooling it to about 100 K before attaining the mirror, to further reduce the heat load.

The metal atom source was completely enclosed inside another liquid nitrogen-cooled trap minimizing greatly the thermal radiation and outgassing impurities. A tungsten filament, wetted with Co (Alfa Aesar, Germany, 99.995%), was heated at 1400−1600 °C to generate the metal vapor. The metal deposition rate was monitored with the aid of a quartz microbalance[15] and varied from 9 to 20 nanomol/min.

High-purity neon (Air Liquide, 99.995%), $^{16}O_2$ (Air Liquide, 99.998%), and $^{18}O_2$ (Isotec, 99.0% ^{18}O), were used to prepare the O_2−Ne mixtures. To prepare scrambled oxygen ($^{16}O^{18}O$), equal quantities of $^{16}O_2$ and $^{18}O_2$ were mixed and submitted to a Tesla discharge. Absorption spectra were recorded between 30 000 and 80 cm^{-1} on the *same* samples using a Bruker 120 FT spectrometer. CaF_2, KBr, and polyethylene wedged windows were mounted on a rotatable flange separating the interferometer vacuum (10^{-3} mbar) from that of the cryostatic cell (10^{-8} mbar). In the far-IR, (80−500 cm^{-1}) a globar (Si−C) was used, with a composite beam splitter, a polyethylene window, and a He-cooled Si−B bolometer. For the mid-IR region (500−5000 cm^{-1}), a Ge/KBr beam splitter with a KBr window was used along with a liquid N_2-cooled narrow band HgCdTe photoconductor. For the near-IR (4500−9000 cm^{-1}), a tungsten filament source, Si/CaF_2 beam splitter and window, and liquid N_2-cooled InSb or room-temperature InGaAs photodiodes were used. Finally, for the 8000−16 000 and 15 000−30 000 cm^{-1} visible regions, spectra were acquired using TiO_2/quartz beam splitters, a blue- or red-enhanced Si photodiode, and either a W-filament or a Xe short arc source in combination with Schott BG38 or VG9 colored glass filters. The resolution was varied from 0.02 to 1 cm^{-1}.

Results

Co + O_2 reaction products were first isolated in solid argon at 9 K. No CoO molecules were detectable in our experiments then, though bands at 846.2 and 808.6 cm^{-1} had been observed by Andrews et al.[16] and assigned to the fundamental vibrations of ground-state $Co^{16}O$ and $Co^{18}O$ molecules, respectively. When we investigated the same system in solid neon, several bands were present that had so far not been observed in argon. Among all of them, those concerning the CoO molecule will be discussed hereafter; the ones concerning other reaction products will be presented in later papers.

Here in solid neon, using $^{16}O_2$ precursor, two absorption bands, at 849.9 and 851.2 cm^{-1} were observed immediately after deposition (Figure 1). They did not increase after irradiation and only decreased on annealing to 11.5 K. As the samples were deposited at growing temperatures of 3.5, 5.5, and 6.5 K, these bands increased drastically with identical behaviors intensitywise. They showed an isotopic shift of 37.7 cm^{-1} each when $^{18}O_2$ was used, which indicated that these were in fact two different trapping sites of the same species. In the ($^{16}O_2$ + $^{18}O_2$) and ($^{16}O_2$ + $^{16}O^{18}O$ + $^{18}O_2$) isotopic mixtures, the same multiplets were observed showing an isotopic doublet structure characteristic of mono-oxygenated molecules. Irradiating in the visible region or annealing the samples produced small changes in intensity between the different trapping sites. Several new sites started to appear around the two main ones, but the overall integrated intensity barely varied. According to these observations, we attribute these bands to CoO in slightly different trapping sites, and from hereon, for clarity purposes, we will retain the main site value, 851.2 cm^{-1}, as the ground-state fundamental band for CoO in solid neon, because it is the narrowest absorption (fwhm = 0.05 cm^{-1}) and has the frequency closest to that of the gas-phase CoO (851.7 cm^{-1}).

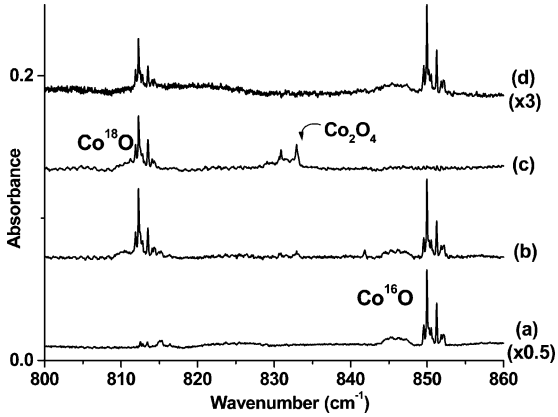

Figure 1. Infrared spectra in the 800−860 cm^{-1} region for thermally evaporated Co atoms codeposited with 500 ppm of O_2 in neon at 6 K. CoO fundamental stretching mode with different isotopic mixtures. (a) Co + $^{16}O_2$, (b) Co + (50% $^{16}O_2$ + 50% $^{18}O_2$), (c) Co + $^{18}O_2$, (d) Co + (25%$^{16}O_2$ + 50%$^{16}O^{18}O$ + 25%$^{18}O_2$).

Four other band systems were observed in the mid- and near-IR region, and the frequencies are reported in Table 1, where we refer to the different systems as A, B, C, and D before any state attribution can be made (Figures 2−5). All systems are present after deposition, but the product yield relative to larger oxides could be varied by more than an order of magnitude, when changing cobalt and oxygen concentrations and experimental conditions. A and B system bands are split into two main signals and many closely spaced less intense ones, in the same manner as the 851.2 cm^{-1} absorption region. All bands show parallel evolutions following irradiations in the green and red and also decrease on annealing. Systems C and D are much weaker but behave like the other two, only showing slightly different trapping site effects with one main peak and three smaller ones around it. None of these systems appears in blank samples containing only cobalt and neon atoms and therefore belong to a cobalt oxide.

Oxygen isotopic substitution was employed for band identification. In the samples containing only $^{18}O_2$ molecules, the first and most intense components of systems A and B were slightly blue-shifted (≈0.7 and 1.6 cm^{-1}), but the second and third set of bands of each system were clearly red shifted by −36.3, −33.9, and −67.2 cm^{-1}, respectively (Figures 2 and 3). System C and D showed larger blue shifts of 2.2 and 3.6 cm^{-1} on the first band and red shifts of −30.1 and −24 cm^{-1} for the second band (Figures 4 and 5). When using ($^{16}O_2$ +$^{18}O_2$) and ($^{16}O_2$ + $^{16}O^{18}O$ + $^{18}O_2$) mixtures, no supplementary bands appeared in any of the systems in addition to those already observed with either $^{16}O_2$ or $^{18}O_2$, confirming that the molecule contains only one oxygen atom.

In very diluted samples deposited at a temperature below 4 K, where CoO was barely formed, the intensities of all four systems varied proportionally to that of the CoO ground-state vibration. Interestingly, in samples grown at more elevated temperatures (5.3−6.5 K), the formation of CoO was favored, and all these bands grew strongly. Irradiations in the visible range and annealing the samples also produced the same intensity changes in all these systems. For these reasons, as well

TABLE 1: Frequencies (cm^{-1}) and Relative Intensities (in parentheses) for Ground State Vibrations and Excited States Vibronic Transitions of $Co^{16}O$ and $Co^{18}O$ Isolated in Solid Neon in the Mid-IR, Near-IR, and Visible Regions

ν_X (0.01)	A (0.51)	B (1)	C (0.01)	D (0.001)	E
		$Co^{16}O$			
849.9/	**3320.2/3376.7**[c]	5755.4/**5808.2**[c]	**6962.1** (1)[c]	**10013.2**/	**17008**[d]
851.2[a,b]	(1)	(1)		10110.3	**17540**
		6547.6/**6601.6**	**7680.8** (0.29)	(1)	**18073**
	4142.6/**4201.2**	(0.18)			**18597**
	(0.02)	7328.9/**7383.6**	**8388.7** (0.05)	**10636.8**	**19126**
		(0.003)		(0.34)	**19647**
		8099.3/**8155.3**			**20170**
		(0.002)			**20690**
					21200
		$Co^{18}O$			
812.3/	3321.0/**3377.6**	5757.2/**5809.8**	**6964.0**	**10016.8**/	
813.5				10113.8	
	4106.5/**4164.9**	6514.1/**6567.7**	**7650.7**		
				10612.8	
		7260.8/**7316.4**	**8328.1**		
		7998.5/**8054.1**			

[a] Main trapping sites are in bold. [b] Uncertainty ±0.01 cm^{-1}. [c] Uncertainty ±0.2 cm^{-1}. Relative intensities with respect to the most intense component of each system. [d] Uncertainty ±3 cm^{-1}.

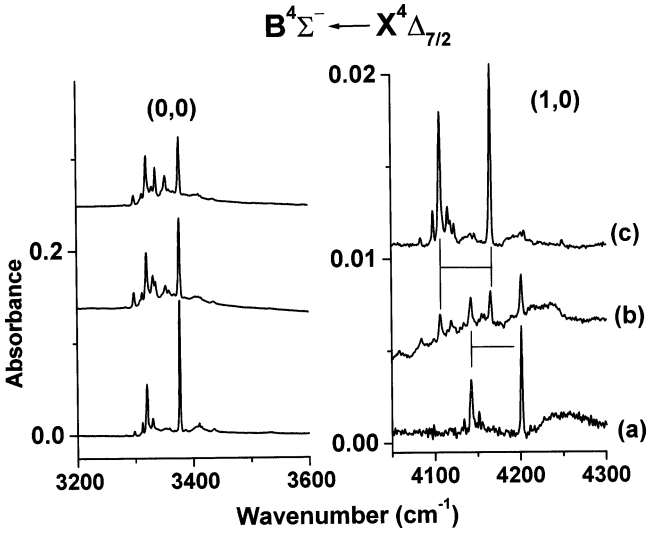

Figure 2. Infrared spectra in the 3200−3600 and 4050−4300 cm^{-1} regions for thermally evaporated Co atoms codeposited with 500 ppm of O_2 in neon at 6 K. Vibronic transitions for system A, ($B^4\Sigma^-$ state), with different isotopic mixtures (a) Co + $^{16}O_2$, (b) Co + 50%$^{16}O_2$ + 50%$^{18}O_2$, (c) Co + $^{18}O_2$.

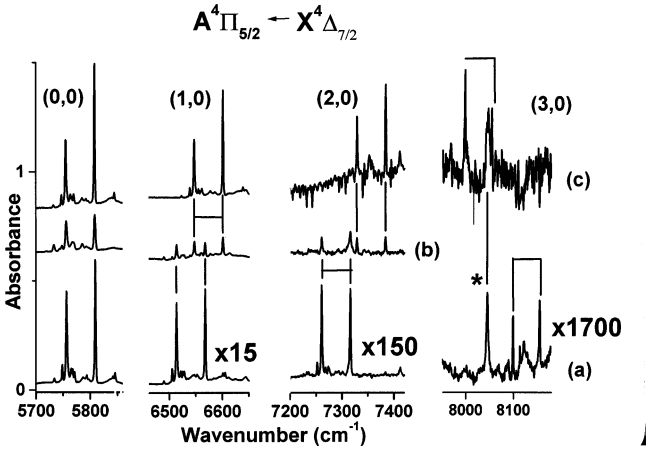

Figure 3. Infrared spectra in the 5700−5850, 6460−6650, 7250−7350, and 7950−8200 cm^{-1} regions for Co atoms codeposited with 500 ppm of O_2 in neon at 6 K. Vibronic transitions for system B ($A^4\Pi_{5/2}$ state), with different isotopic mixtures. * designates an absorption not pertaining to CoO. (a) Co + $^{16}O_2$, (b) Co +50% $^{16}O_2$ +50% $^{18}O_2$, (c) Co + $^{18}O_2$.

as because of the observed isotopic structures, we think that the reported systems all belong to the same species, CoO.

Despite its great complexity, the electronic spectrum of $Co^{16}O$ in the visible region has also been of interest to us. Results for $Co^{16}O$ in solid neon cannot be expected to bring further detail in this already thoroughly studied region,[3,4,7] but it was nevertheless reinvestigated to facilitate the consistency of comparisons between solid Ne matrix and the gas phase. As might be anticipated, the solid neon samples containing $Co^{16}O$ molecules presented absorptions covering the whole 13 500−22 000 cm^{-1} region. The total integrated intensity is roughly 15 times that of the strong band system near 5800 cm^{-1} reported earlier (system B) and indicates the presence of several fully allowed electronic transitions covering this region. The spectral features here are very broad compared to those in the mid- or near-IR, and congestion is quite extreme. In the red, onsets of several progressions seem discernible near 13 835, 14 660, and 15 440 cm^{-1}, with first spacings of about 580, 612, and 650 cm^{-1}. Unfortunately, the progression patterns appear either to be very irregular or to blend together too rapidly to allow analysis.

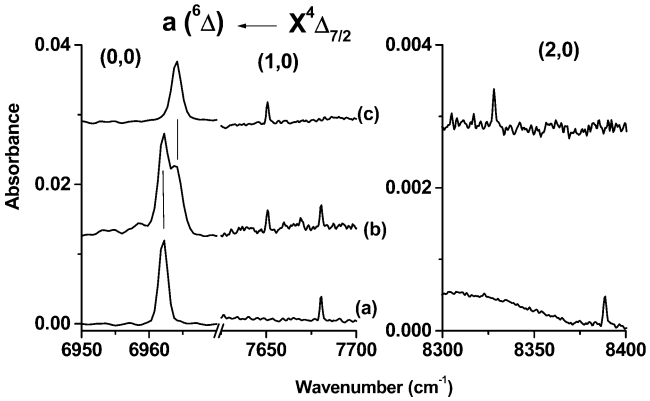

Figure 4. Infrared spectra in the 6940−6980 and 7640−7700 cm^{-1} regions for thermally evaporated Co atoms codeposited with 500 ppm of O_2 in neon at 6 K. Vibronic transitions for system C (a($^6\Delta$)? state), with three different isotopic mixtures. (a) Co + $^{16}O_2$, (b) Co +50% $^{16}O_2$ + 50% $^{18}O_2$, (c) Co + $^{18}O_2$.

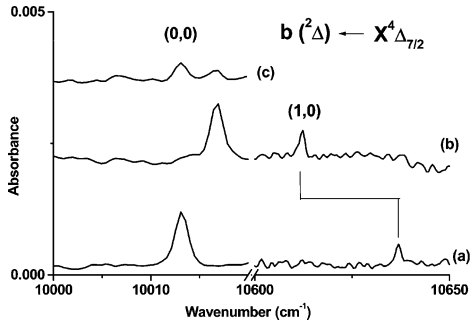

Figure 5. Infrared spectra in the 10000−10650 cm^{-1} region for thermally evaporated Co atoms codeposited with 1000 ppm O_2 in neon at 6 K. Vibronic transitions for system D (b($^2\Delta$)? state), with different isotopic mitures. (a) Co + $^{16}O_2$, (b) Co + $^{18}O_2$, (c) Co +(49% $^{16}O_2$ + 42% $^{16}O^{18}O$ + 9% $^{18}O_2$).

Above 17 000 cm^{-1} more recognizable patterns begin to emerge, with parallel series of absorptions having comparable line shapes and also progressively increasing and then decreasing intensities. More specifically, a series of relatively well-defined absorptions at 17 008, 17 540, 18 073, 18 597, 19 126, 19 647, 20 170, 20 690, and 21 200 cm^{-1} follows a consistent behavior throughout the experiments and matchs that of the main trapping site defined above for the other mid- and near-IR band systems of Co^{16}O. These peaks remain much broader (fwhm ∼ 20 cm^{-1}) than those of the other systems, and the uncertainty on the frequency determination is estimated to ±3 cm^{-1} for the seven strongest bands. This system will be referred to as system E in Table 1. Other parallel progressions appear with comparable patterns and behaviors traceable to that of the minor trapping sites of Co^{16}O and will not be considered further.

A second set of absorptions centered around 17 770, 18 360, 18 900, 19 400, 19 900, and 20 550 cm^{-1} is also observable. It is interleaved with the one mentioned previously, and the line shapes are once again broad and irregular. The increasing complexity throughout this progression makes any attempted spectroscopic analysis impossible, and we will not try to extract data from this system.

Discussion

The structures of the A, B, C, and D systems suggest vibrationaly resolved electronic transitions. No rotation is possible in the matrix for this molecule, due to its size, but temperature effects do leave signs of possible libration as profile and peak frequency vary reversibly with the temperature between 3.8 and 9.5 K and differ slightly from site to site. Through these effects (temperature and annealing) we can correlate each site of the vibronic transition to a site of the ground-state fundamental vibration. The 849.9 cm^{-1} band, the most intense of the two sites of the ground state fundamental, correlates clearly with the 3320.2 and 4142.6 cm^{-1} bands of system A and the 5755.4, 6547.6, 7328.9, and 8099.3 cm^{-1} bands of system B, which are all the least intense of the doublet components. Conversely the 851.2 cm^{-1} band, which is the least intense of the two main absorptions in the mid-IR, correlates with the 3376.7 and 4201.2 cm^{-1} bands of system A and the 5808.2, 6601.6, 7383.6, and 8155.3 cm^{-1} bands of system B, which are all the most intense in the vibronic absorptions. (Figures 2 and 3)

Since the 851.2 cm^{-1} band was retained as the reference value for the fundamental vibration of ground state CoO in Ne, for clarity we will only consider in the discussion the bands correlating with the 851.2 cm^{-1} site. All spectroscopic constants deduced hereafter are obtained taking only those main absorptions into account.

System B (Figure 3). This is the most intense of the three systems; it is vibrationaly resolved showing up to three vibrational levels in the excited state. The 5808.2 cm^{-1} band shows a small blue shift upon oxygen isotopic substitution and is a purely electronic transition B(v'=0) ← $X^4\Delta$(v'' = 0). The 6601.6, 7383.6, and 8155.3 cm^{-1} bands, on the other hand, show isotopic shifts of $\Delta\nu$ = −33.9, −67.2, and 101.2 cm^{-1} in samples containing $^{18}O_2$ precursor. These bands correspond to the B(v'=1, 2 or 3) ← $X^4\Delta$(v''=0) transitions. With only a quadratic term for the anharmonicity, one obtains the harmonic frequency ω_e = 804.8 cm^{-1}, the anharmonicity, $\omega_e x_e$ = 5.7 cm^{-1}, and ±0.6 cm^{-1} deviation in the $\Delta G_{(v+1/2)}$ frequency reproduction, somewhat larger that the experimental uncertainty. Adding a cubic term improves the fit but gives values marginally different (ω_e = 805.8 cm^{-1}, $\omega_e x_e$ = 6.5 cm^{-1}, and $\omega_e y_e$ = 0.18 cm^{-1}). Using ground-state data[4] (ω_e = 862.4 cm^{-1}, $\omega_e x_e$ = 5.13 cm^{-1}) the electronic transition energy T = 5837 cm^{-1} (0.73 eV) is obtained. A simple calculation, using the well-known relation for the Morse potential would predict D_e ≈ 28 400 cm^{-1}, compared to 36 200 cm^{-1} in the ground state.

Ram et al.[6] reported a complete study of the 0−0 band of the $A^4\Pi_{5/2}$−$X^4\Delta_{7/2}$ transition near 5776 cm^{-1} observed through emission spectroscopy. System B is thus shifted by about 32 cm^{-1} (0.5%) compared to the gas-phase value, which is well in the range of usual neon-to-gas shift.[17] Noting that the molecule displays some Hund's case c tendencies, Ram et al.[6] still based their discussion within Hund's case a formalism; here intensities are consistent with this being an allowed transition ($\Delta\Lambda$ = 1, ΔS = 0). So system B is thus attributed to the $A^4\Pi_{5/2}$(v'=0,1,2,3) ← $X^4\Delta_{7/2}$(v'',0) transitions.

System A (Figure 2). As shown in Figure 2, in the $^{18}O_2$/Ne samples, the 3376.7 cm^{-1} band is slightly blue-shifted (0.8 cm^{-1}), thereby indicating a purely electronic transition A(v'=0) ← $X^4\Delta$(v''=0), whereas the 4201.2 cm^{-1} band is red shifted by −36.3 cm^{-1}, indicating a vibronic transition A(v'=1) ← $X^4\Delta$(v''=0). The upper state seems to be the lowest lying $^4\Sigma$ excited state of CoO, first predicted by Dolg et al.[9] 0.52 eV above the ground state. We assign these transitions to $B^4\Sigma_{3/2}$(v'=0,1) ← $X^4\Delta_{7/2}$ (v''=0) following the notations used by Barnes et al.[7]

Taking an average of the anharmonicities in the $X^4\Delta_{7/2}$ and $A^4\Pi_{5/2}$ states ($\omega_e x_e$ = 5.13 and 5.70 cm^{-1}, respectively) we obtain T = 3390 cm^{-1} for the electronic transition energy and ω_e = 835.5 cm^{-1} for the vibrational harmonic frequency in the $B^4\Sigma^-$ state. To establish a fair comparison with the ab initio results,[10,13] two corrections must be made. First, averaging the energies of the four spin−orbit components of the ground state and neglecting the small spin−spin interactions of the $B^4\Sigma^-$ state will reduce T to about 2840 cm^{-1}. Next, applying the same 0.5% neon-to-gas shift as for the $A^4\Pi_{5/2}$ ← $X^4\Delta_{7/2}$ transition will rescale it up to about T = 2855 cm^{-1} (0.35 eV). In the latest predictions of Uzunova et al.,[13] this value was calculated at 0.42 eV, in better agreement with our results. However, they also calculated a harmonic frequency of ω_e = 913 cm^{-1}, larger than that of the $X^4\Delta_{7/2}$ ground state (885 cm^{-1}) and opposed to the 26.7 cm^{-1} decrease observed here.

It is interesting to compare the intensities of this system with those of the $A^4\Pi_{5/2}$ ← $X^4\Delta_{7/2}$ transition, the latter being completely allowed ($\Delta\Lambda$ = 1, ΔS = 0). Indeed, the disobeyed selection rules should not influence the intensities in the same way. The $B^4\Sigma$ ← $X^4\Delta_{7/2}$ transition is forbidden for Hund's case a molecules, since $\Delta\Lambda$ = 2, even if ΔS = 0 is respected, but the transition is allowed in case c. It is here observed about half as intense as the $A^4\Pi_{5/2}$ ← $X^4\Delta_{7/2}$ transition.

TABLE 2: Molecular Parameters for CoO Isolated in Neon

	$X^4\Delta_{7/2}$[a]	$B^4\Sigma^-$	$A^4\Pi_{5/2}$	a($^6\Delta$?)	b($^2\Delta$?)	$E^4\Delta$
T (cm^{-1})[a]		3390	5837	7028	10131(±5)[e]	15446(±8)
(eV)	0	0.42	0.73	0.87	1.26	1.93
$\nu(0\rightarrow1)$[b]	**851.2**	**824.5**	**793.4**	**718.8**	**623.6**	
ω_e (cm^{-1})	862.4[c]	835.5[d]	804.8	729.7		540(±10)
$\omega_e x_e$ (cm^{-1})	5.13[c]	5.4[d]	5.7	5.45		3(±2)

[a] Uncertainty ±1.2 cm^{-1}. [b] Uncertainty ±0.4 cm^{-1}. [c] Values obtained by Barnes et al.[7] in the gas phase. [d] Supposing an average value for the anharmonicity between $X^4\Delta_{7/2}$ and the $A^4\Pi_{5/2}$ state values.

Systems C and D (Figures 4 and 6). System C, 2 orders of magnitude less intense than system A, is likely to involve a change in the spin multiplicity but may respect $\Delta\Lambda = 0,\pm1$ and the upper electronic state will thus be labeled "a". When using ^{18}O, the first transition, which is expected to be purely electronic, presents a slight blue shift of 2.2 cm^{-1}, which signals a significant change in the profile of the potential energy function, inducing also strong variation in the vibrational frequency. The bands at 6962.1, 7680.8, and 8388.7 cm^{-1} are assigned to a(v'=0,1,2) ← $X^4\Delta_{7/2}$ (v''=0) transitions. $\Delta G_{1/2}$ = 718.7 cm^{-1} for this state, compared to 851.2 cm^{-1} in the ground state, a 15% variation showing a larger change in the bond length than for the $B^4\Sigma$ or $A^4\Pi$ states. This larger geometry change induces different Franck−Condon factors and a smoother intensity decrease between the (0,0), (1,0), and (2,0) bands than in systems A and B. From these data, one obtains ω_e = 729.7 cm^{-1}, $\omega_e x_e$ = 5.45 cm^{-1}, and T = 7028 cm^{-1}.

System D is also much weaker than system A by several orders of magnitude, thus likely to involve a change in spin multiplicity, and the upper state will be labeled "b". Only the first two members of the vibrational progression have been observed and display the same tendencies as for sytem C. The 10 013.2 and 10 636.8 cm^{-1} bands are thus assigned to b(v'=0,1) ← $X^4\Delta_{7/2}$ (v''=0) transitions. $\Delta G_{1/2}$ = 623.6 cm^{-1} for this state, and we estimate T = 10 131 ± 5 cm^{-1}, in absence of an anharmonicity estimate.

Uzunova et al.[13] calculated the $^6\Delta$ and $^2\Delta$ states 0.8 and 1 eV above the GS, respectively. Without gas-phase data allowing estimates of the spin−orbit splitting for these states, this effect (possibly nonnegligible, $X^4\Delta_{7/2}-X^4\Delta_{1/2} \approx 1150$ cm^{-1})[4] cannot be taken into account in the total energies, and the shift induced by the neon matrix is also not exactly known here. But, if once again we consider a 0.5% shift as for the $A^4\Pi-X^4\Delta$ transition, we obtain 0.87 and 1.25 eV, corrected from the matrix shift. The predicted harmonic vibrational frequencies, 769 cm^{-1} for the $^6\Delta$ state and 576 cm^{-1} for the $^2\Delta$ state,[13] can also be compared favorably to the $\Delta G_{1/2}$ = 719 and 623.6 cm^{-1} obtained in our experiments; therefore, systems C and D are tentatively assigned to $a^6\Delta \leftarrow X^4\Delta_{7/2}$ and $b^2\Delta \leftarrow X^4\Delta_{7/2}$, respectively.

In the work of Barnes et al.,[7] electronic configurations for the ground state and the first five electronic excited states were proposed. In order of growing energy the states were as follows: $X^4\Delta_{7/2}$ ($\sigma^2\delta^3\pi^2$), $B^4\Sigma^-$ ($\sigma\delta^4\pi^2$), $A^4\Pi$ ($\sigma^2\delta^2\pi^3$), $^4\Phi$ ($\sigma\delta^3\pi^3$), $^6\Delta$ ($\sigma\delta^3\pi^2\sigma$), and $D^4\Phi$ ($\sigma^2\delta^3\pi\sigma$), the latter being in the visible region. This comforts us in the possible attribution of system C to the $a^6\Delta(v'=0,1) \leftarrow X^4\Delta_{7/2}(v''=0)$ transitions. Looking at the excited-state frequencies (Table 2), changes are substantial in the values from the $A^4\Pi_{5/2}$ to the $a^6\Delta$ compared to the lower states, which implies that there might be a significant change in orbital occupation with an antibonding HOMO and no longer just nonbonding. According to the work of Bauschlicher and Maitre,[10] the metal s−d hybrid orbitals give rise to a nonbonding σ orbital, and since the oxygen has no occupied δ orbital, the metal 3dδ is nonbonding. So the order of stability suggests that σ and 3dδ are nonbonding while 3dπ and 3dσ are antibonding. Therefore, this frequency change is consistent with a larger "antibonding character" for the LUMO 3dσ orbital than the HOMO 3dπ.

System E. Barnes et al.[7] have rovibrationally analyzed the $D^4\Phi-X^4\Delta$ as well as C-, E-, and $F^4\Delta-X^4\Delta$ transitions in the visible range. In this study, the great complexity due to the presence of several overlapping electronic states was analyzed in detail with powerful means, and the difficulty of following the nonmonotonic variations of the vibrational intervals was a clear sign of considerable interactions between the various electronic states. Data obtained with jet-cooled CoO and LIF excitation spectra in this region first show progressions belonging to $C^4\Delta-X^4\Delta$ with onset at 13 950 cm^{-1}, next to $D^4\Phi-X^4\Delta$, starting at 14 612 cm^{-1} and E- and $F^4\Delta-X^4\Delta$ band systems with onsets at 15 242 and 15 651 cm^{-1}, respectively. The authors noted that the red and orange regions involving the first two transitions and the onset of the next two are very confused, and interactions between various states cause erratic vibrational spacing and intensity variations. The broad and complex absorption systems starting near 13 837 and 14 660 cm^{-1} in neon can possibly correspond to the first two band systems, but we cannot be more affirmative.

Above 17 000 cm^{-1}, the progressions due to the first two transitions die out rapidly, and only the E- and $F^4\Delta-X\ ^4\Delta$ band systems give rise to long progressions, heavily complicated by several kinds of perturbations. System E, a set of relatively well-defined absorptions at 17 008, 17 540, 18 073, 18 597, 19 126, 19 647, 20 170, 20 690, and 21 200 cm^{-1} indicates an average vibrational spacing of 526 cm^{-1}, clearly in better agreement with what is deduced in the gas phase for the E−X system (ν ~ 524 cm^{-1}) than for the F−X system (above 600 cm^{-1}). Comparison thus suggests attribution of the observed sequence in neon to the E−X(v,0) bands, with v = 3−11, which now provides a reasonable match, assuming a total, matrix-to-gas blue shift of about 160 cm^{-1} on the first members of the progression (almost 1%, to be compared to about 0.5% for the IR band system B). Note that the increase of the vibrational spacing above v = 8 explained in ref 7 as a sign of interaction with a perturbing state is not observed in neon, likely due to quenching of the coupling mechanism by interaction with the matrix. A simple analysis of our data suggests that T_0 = 15 446 ± 8 cm^{-1} in neon, ω_e = 540 ± 10 cm^{-1}, and $\omega_e x_e$ = 3 ± 2 cm^{-1}, to be compared to T_0 = 15 242 cm^{-1}, ω_e = 535.6 cm^{-1}, and $\omega_e x_e$ = 5.5 cm^{-1} for the $E^4\Delta$ state of CoO in the gas phase, uncertainties being defined as three times the rms deviation. It can thus be concluded that the matrix-induced perturbation on vibrational frequencies, even on this highly excited state, can be considered small enough to be neglected next.

Correlation between Force Constants and Bond Distances in CoO. In the chemistry field, an important use of spectroscopy is to derive relationships between spectroscopic and structural parameters. In light of these and previous results on the CoO molecule, we would like to present a relative correlation between bond lengths and force constants. All data considered, we have information on six electronic states, including the ground state, which are, in order of growing energy: $X^4\Delta_{7/2}$, $B^4\Sigma$, $A^4\Pi_{5/2}$, a($^6\Delta$?), b($^2\Delta$?), and $E^4\Delta$. The $E^4\Delta$ and $X^4\Delta_{7/2}$ states thoroughly studied in the gas phase are used as cornerstones to evaluate matrix-induced deviations on the bond length (r_e). The $A^4\Pi_{5/2}$ has also been characterized in the gas phase,[6] but the vibrational frequency for this state has not yet been supplied, and we will therefore use the one obtained here in solid neon.

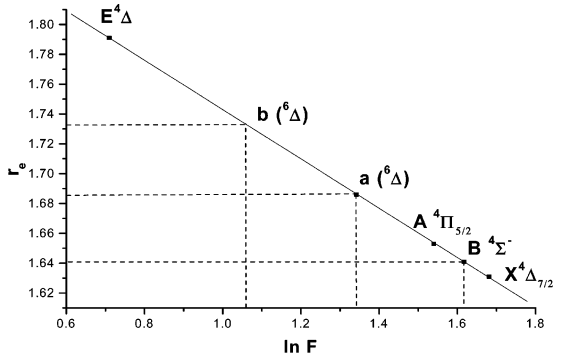

Figure 6. Hershbach and Laurie's rule plot of r_e vs ln (F), where F is the harmonic force constant. Explicit values are reported Table 3, and gas phase values are taken from refs 3, 6, and 7.

The first possibility was to fit the data according to Badger's rule, not in its original form, $k_e(r_e - d_{ij})^3 = 1.86$ mdyn Å^2,[18] but in the optimized form by Weisshaar[19] more specific to transition metal oxides, $k_e(r_e - d_{ij})^3 = 1.09$ mdyn Å^2, where d_{ij} is still the empirical "distance of nearest approach" dependent on the rows i and j of the atoms. In this revisited case $d_{ij} = d_{13} = 0.47$ Å, obtained through the linear form of the equation and deduced from the intercept. This equation has proven to be quite effective for many molecules and supplied results as acceptable as those obtained through quantum chemical calculations,[20] but in the case of CoO, this equation gave unsatisfactory results. The error for the ground-state force constant, though it was the smallest one, is already 9.5% (5.91 mdyn Å^{-1} calculated for 5.37 mdyn Å^{-1} obtained experimentally in the gas phase), and the error on the excited states goes up to 100% in the highly excited states such as the $E^4\Delta$ (4.01 mdyn Å^{-1} calculated for 2.03 mdyn Å^{-1} experimentally). Rather, to relate bond lengths and force constants we will use the Herschbach and Laurie[21] equation for diatomic molecules, which has a slightly broader scope

$$(-1)^n F_n = 10^{-(r_e - a_{ij})/b_{ij}} \quad \text{or} \quad r_e = a_{ij} - \frac{b_{ij}}{2.3} \ln F_n$$

where F_n is the n^{th} order of the force constant, r_e is an average internuclear equilibrium distance, and a_{ij} and b_{ij} are constants dependent on the rows i and j of the atoms involved. This method appears to be the most accurate for these types of systems, because it is more general. It allows calculation of several orders of the force constant and thereby a better precision. The data on the $E^4\Delta$, $A^4\Pi_{5/2}$, and $X^4\Delta_{7/2}$ states in the gas/matrix phases will be used to determine the a_{ij} and b_{ij} constants for CoO and r_e for the $B^4\Sigma$ and $a^6\Delta$ states, in accordance with the observed vibrational frequencies (Figure 6). Results are reported Table 3 along with the calculated values by Uzunova et al.[13] for comparison.

The equation provides $a_{ij} = 1.910$ Å (±0.002) and $b_{ij} = 0.380$ (±0.001) (Figure 6) and can be compared to the general a_{13} and b_{13} obtained by Herschbach and Laurie [21] equal to 2.15 and 0.60, respectively, which represent average values over several very different diatomic molecules. Our determination of these constants is more specific to CoO on which no data existed at the time. Nonetheless, and given the acceptable degree of approximation brought by this method, it gives a good indication of the bond length evolution with the force constant. The interatomic distances interpolated for the $B^4\Sigma$, a($^6\Delta$?), and b($^2\Delta_?$) states are respectively 1.64, 1.69, and 1.73 ± 0.01 Å. The uncertainty is estimated using the matrix value of the effective force constant (F_2) for the $E^4\Delta$ state on the graph and obtaining thereby an effective bond length that is only within 0.01 Å of the value obtained using the gas-phase frequency.

TABLE 3: Comparison of Observed and Estimated Parameters for Various Electronic States of CoO

	frequency (cm^{-1})			force constant (mdyn Å^{-1})		r_e (Å)	
electronic states	gas	neon matrix	calcd[a]	gas	neon matrix	expl[b]	calcd[a]
$X^4\Delta_{7/2}$	851.7	851.2	885	5.375	5.369	1.631[b]	1.629
$B^4\Sigma^-$		824.5	913		5.038	1.641[c]	1.597
$A^4\Pi_{5/2}$		793.4			4.665	1.653[b]	
a($^6\Delta$?)		718.8	769		3.829	1.686[c]	1.667
b($^2\Delta$?)		623.6	576		2.886	1.733[c]	1.734
$E^4\Delta$	524.6	534		2.034	2.161	1.791[b]	

[a] DFT results from ref 13, calculated harmonic vibrational frequency ω. [b] Gas-phase data from refs 3, 6, and 7. Gas phase-to-matrix shift on r_e is on the order of ±0.01 Å. [c] Obtained through Herschbach and Laurie linear regression.

As discussed previously, predictions by Barnes et al.[7] have a $^4\Phi$ state lying between the $A^4\Pi_{5/2}$ and the $a^6\Delta$, and though we do not observe it, the leap in frequencies could be explained by a considerable electronic configuration change.

Conclusions

In this paper, we presented new data on vibrationally resolved electronic transitions of CoO isolated in solid neon in the mid- and near-IR region. These systems have origins around 3400, 5800, 7000, and 10 000 cm^{-1}. Comparison with gas-phase data[6] enable assignment of the upper state of the second vibronic system to the $A^4\Pi_{5/2}$ state. Assignments of the first, third, and fourth excited states to $B^4\Sigma$, $a^6\Delta$, and $b^2\Delta$ are suggested by comparisons with DFT calculations,[13] but are tentative in absence of gas-phase data. For the first three excited states, harmonic frequencies and anharmonicities can been estimated. Matrix-induced perturbations have been taken into consideration and can be determined on the $A^4\Pi$ and $E^4\Delta$ energies, representing a 0.5% to 1% blue shift.

Using a Herschbach and Laurie[21] relation correlating bond length and force constant for CoO, we fitted the data including the $X^4\Delta_{7/2}$ ground state and the excited $A^4\Pi_{7/2}$ and $E^4\Delta$ states, combining gas phase and neon matrix data, and submit a first estimation of the bond lengths for the $B^4\Sigma^-$, a($^6\Delta$?) and b($^2\Delta$?) excited states. The uncertainty on the internuclear distance has been estimated at ±0.01 Å in comparison with the gas phase. Further gas-phase studies will be needed in order to shed more light on the complicated spectra of CoO in the IR region and bring yet better understanding of this system.

Acknowledgment. We thank Danielle Carrère for her careful assistance in preparing the experiments and Simon Fourquet for his contribution in preparing some samples. This work was supported by CNRS Grant UMR 7075, and equipment was purchased with the help of Plan Pluri-Formation of the University Pierre et Marie Curie.

References and Notes

(1) Green, D. W.; Reedy, G. T.; Kay, J. G. *J. Mol. Spectrosc.* **1979**, *78*, 257.

(2) Weltner, W., Jr. *Ber. Bunsen-Ges.* **1978**, *82*, 80.

(3) Adam, A. G.; Azuma, Y.; Barry, J. A.; Huang, G.; M. P. J. Lyne, M. P. J.; A. J. Merer, A. J.; Schröder, J. O. *J. Chem. Phys.* **1987**, *86*, 10, 5231.

(4) Clouthier, D. J.; Huang, G.; Merer, A. J.; Friedman-Hill, E. J. *J. Chem. Phys.* **1993**, *99*, 9, 6336.

(5) Namiki, K. C.; Saito, S. *J. Chem. Phys.* **2001**, 114, 21, 9390.

(6) Ram, R. S.; Jarman, C. N.; Bernath, P. F. *J. Mol. Spectrosc*. **1993**, *160*, 574.
(7) Barnes, M.; Clouthier, D. J.; Hajigeorgiou, P. G.; Huang, G.; Kingston, C. T.; Merer, A. J.; Metha, G. F.; Peers, J. R. D.; Rixon, S. J. *J. Mol. Spectrosc*. **1997**, *186*, 374.
(8) Krauss, M.; Stevens, W. J. *J. Chem. Phys*. **1985**, *82*, 5584.
(9) Dolg, M.; Wedig, U.; Stoll, H.; Preuss, H. *J. Chem. Phys*. **1987**, *86*, 2123.
(10) Bauschlicher, C. W., Jr.; Maitre, P. *Theor. Chim. Acta* **1995**, *90*, 189.
(11) Bridgeman, A. J.; Rothery, J. *J. Chem. Soc., Dalton Trans*. **2000**, 211.
(12) Gutsev, G. L.; Rao, B. K.; Jenna, P. *J. Phys. Chem*. A **2000**, *104*, 5374.
(13) Uzunova, E. L.; Nikolov, G. St.; Mikosch, H. *J. Phys. Chem*. A **2002**, *106*, 4104.
(14) Dai, B.; Deng, K.; Yang, J.; Zhu, Q. *J. Chem. Phys*. **2003**, *118*, 21, 9608.
(15) Huner, B.; Klinkhachorn, P.; Overton, E. B. *Rev. Sci. Instrum*. **1988**, *59*, 983.
(16) Chertihin, G. V.; Citra, A.; Andrews, L.; Bauschlicher, C. W., Jr. *J. Phys. Chem.* A **1997**, *101*, 8793.
(17) Jacox, M. E. *J. Mol. Struct.* **1987**, *157*, 43.
(18) Badger, R. M. *J. Chem. Phys*. **1934**, *2*, 128; **1935**, *3*, 710.
(19) Weisshaar, J. C. *J. Chem. Phys.* **1989**, *90*, 3, 1429.
(20) Cioslowski, J.; Liu, G.; Mosquera Castro, R. A. *Chem. Phys. Lett*. **2000**, *331*, 497.
(21) Herschbach, D. R.; Laurie, V. W. *J. Chem. Phys*. **1961**, *35*, 458.